Cell

Soluble FLT1 Binds Lipid Microdomains in Podocytes to Control Cell Morphology and Glomerular Barrier Function

Jing Jin,[1,14] Karen Sison,[1,14] Chengjin Li,[1] Ruijun Tian,[1] Monika Wnuk,[1] Hoon-Ki Sung,[1] Marie Jeansson,[1] Cunjie Zhang,[1] Monika Tucholska,[1] Nina Jones,[3] Dontscho Kerjaschki,[4] Masabumi Shibuya,[5] I. George Fantus,[2,6,7] Andras Nagy,[1,9] Hans-Peter Gerber,[11] Napoleone Ferrara,[12] Tony Pawson,[1,10] and Susan E. Quaggin[1,8,13,*]

[1]Samuel Lunenfeld Research Institute
[2]The Department of Medicine
Mount Sinai Hospital, Toronto, Ontario M5G 1X5, Canada
[3]Department of Molecular and Cellular Biology, University of Guelph, Guelph, Ontario N1G 2W1, Canada
[4]Department of Pathology, Medical University Vienna, A-1090 Vienna, Austria
[5]Institute of Physiology and Medicine, Jobu University, Takasaki 370-1393, Japan
[6]Toronto General Research Institute, Toronto, Ontario M5G 1L7, Canada
[7]Department of Physiology and Banting and Best Diabetes Centre
[8]Department of Medicine, University Health Network
[9]Department of Obstetrics and Gynaecology
[10]Department of Molecular Genetics
University of Toronto, Ontario M5S 1A8, Canada
[11]BioConjugate/Vascular Biology, Oncology Research Unit East, Pfizer Worldwide Research and Development, Pearl River, NY 10965, USA
[12]Genentech, Inc., South San Francisco, CA 94080, USA
[13]Division of Nephrology, St. Michael's Hospital, Toronto, Ontario M5B 1W8, Canada
[14]These authors contributed equally to this work
*Correspondence: quaggin@lunenfeld.ca
http://dx.doi.org/10.1016/j.cell.2012.08.037

SUMMARY

Vascular endothelial growth factor and its receptors, FLK1/KDR and FLT1, are key regulators of angiogenesis. Unlike FLK1/KDR, the role of FLT1 has remained elusive. FLT1 is produced as soluble (sFLT1) and full-length isoforms. Here, we show that pericytes from multiple tissues produce sFLT1. To define the biologic role of sFLT1, we chose the glomerular microvasculature as a model system. Deletion of *Flt1* from specialized glomerular pericytes, known as podocytes, causes reorganization of their cytoskeleton with massive proteinuria and kidney failure, characteristic features of nephrotic syndrome in humans. The kinase-deficient allele of *Flt1* rescues this phenotype, demonstrating dispensability of the full-length isoform. Using cell imaging, proteomics, and lipidomics, we show that sFLT1 binds to the glycosphingolipid GM3 in lipid rafts on the surface of podocytes, promoting adhesion and rapid actin reorganization. sFLT1 also regulates pericyte function in vessels outside of the kidney. Our findings demonstrate an autocrine function for sFLT1 to control pericyte behavior.

INTRODUCTION

Vascular endothelial growth factor (VEGF) is a major regulator of developmental and pathologic angiogenesis. There are two main cognate receptor tyrosine kinases for VEGF: FLK1/KDR (VEGFR2) and FLT1 (VEGFR1). The classically recognized functions of VEGF, including regulation of endothelial cell migration, proliferation, and differentiation, are mediated by FLK1/KDR. In contrast, the role of FLT1 is not as well understood. Two major splice variants of the *FLT1* gene encode the full-length transmembrane receptor and a soluble, secreted, truncated receptor (soluble FLT1 [sFLT1]) (Shibuya, 2001); the soluble FLT1 messenger RNA (mRNA) is translated into a protein consisting of six Ig repeats and a unique C terminus that retains the ligand-binding domain but lacks the transmembrane and C-terminal tyrosine kinase domains.

sFLT1 is capable of binding all isoforms of VEGF, inhibiting their proangiogenic function. Conventional knockout of the *Flt1* gene in mice results in a lethal vascular phenotype characterized by endothelial cell overgrowth, suggestive of enhanced VEGF activity (Fong et al., 1995). In contrast, mice carrying two modified *Flt1* alleles lacking the cytoplasmic tyrosine kinase signaling domain but retaining the ability to express the soluble *Flt1* isoform are viable with only mild adult phenotypes (Hiratsuka et al., 1998; Niida et al., 2005; Sawano et al., 2001). Together, these results suggest that signaling by FLT1 is non-essential and support a primary role for FLT1 and sFLT1 as

decoy receptors, limiting the availability of VEGF to signal through FLK1/KDR.

In this regard, elevated circulating levels of sFLT1 are associated with pre-eclampsia and characteristic abnormalities in the microvasculature in the kidney (Maynard et al., 2003). Thus, along with its actions to regulate systemic angiogenesis, VEGF and its receptors play a critical role in regulating the development and function of the glomerular filtration barrier in the kidney (Eremina et al., 2003, 2008). The glomerulus is a specialized microvascular bed that is lined by fenestrated, highly flattened endothelial cells. Podocytes function as vasculature support cells or specialized pericytes, extending primary microtubular-based processes and secondary actin-based foot processes around the underlying glomerular capillaries and serving as the main source of VEGF in the glomerulus.

Unexpectedly, we find that podocytes and other perivascular cells from a number of vascular regions produce sFLT1. Thus, we wondered what biologic role(s) sFLT1 plays in pericytes, first focusing on glomerular podocytes as a model system.

RESULTS

Differentiated Pericytes and Perivascular Cells Produce sFlt1

sFLT1 is deposited around mature vessels, suggesting local production occurs away from the circulatory side (Sela et al., 2008, 2011). We screened for expression of *sFLT1* by quantitative PCR (qPCR) in a number of pericyte and perivascular cell lines, as well as endothelial cells (Figure 1A). Pericytes and perivascular cells from the kidney, embryo (10T1/2), retina (Figure 1A), brain, placenta, and liver (data not shown) express full-length and s*FLT1*. To define the in vivo function of FLT1 produced by pericytes, we focused on the glomerular microvasculature and podocytes as a well-characterized vascular bed. Analysis of *sFlt1* as compared to full-length *Flt1* from fluorescence-activated cell sorted (FACS sorted) primary mouse podocytes confirms that sFlt1 is the major isoform produced by podocytes (Figure 1B) (Sison et al., 2010). Moreover, *Flt1* is the only VEGF receptor with detectable expression in podocytes, where it is expressed beginning at 3 weeks and peaking at 6 weeks of age (Figure 1B; Sison et al., 2010). Using immunogold electron microscopy, we find that the Flt1 protein is primarily located at the basal aspect of podocyte foot processes, adjacent to the slit diaphragm (Figure 1C) and in endosomes (data not shown).

Podocyte-Selective Deletion of *Flt1* Results in Cytoskeletal Reorganization and Proteinuria

To determine the function of Flt1 in podocytes in vivo, mice carrying a floxed *Flt1* allele were bred to mice expressing Cre recombinase under control of the podocyte-specific *Nphs1* promoter (Figure 1D; Eremina et al., 2003). In mice carrying two floxed *Flt1* alleles and the Cre transgene (*Nphs1-Cre*$^{+}$ *Flt1*$^{flox/flox}$), proteinuria could be detected at 4 weeks of age (2.3-fold increase over control) that rapidly increases during subsequent weeks (10-fold increase at 8 weeks) (Figure 1E). At 3 weeks of age, before the onset of proteinuria, electron micrographs (EMs) of mutant mice are indistinguishable from controls, demonstrating proper development and formation of foot processes and slit diaphragms (data not shown). At 6 weeks, histologic analysis shows minimal structural changes in the glomerulus by light microscopy but obvious protein casts in tubules (Figure 1F). However, EMs show profound reorganization of podocyte architecture with flattening of foot processes (Figure 1G). Upon aging, glomerular injury progresses with structural changes evident by 8 weeks of age. By 12 weeks, there is evidence of neoangiogenesis, with abnormal blood vessels observed in the urinary space of a small number (<5%) of glomeruli (Figure 1H), but this was a minor feature compared to podocyte defects, indicating a predominant role for direct actions of Flt1 to maintain normal pericyte function.

A Kinase-Deficient *Flt1* Allele Rescues the Phenotype

To determine whether the glomerular defects resulted from loss of the signaling function of Flt1, we used TK mutant mice (*Flt1*$^{TK/TK}$) lacking the cytoplasmic domain and its tyrosine residues, but retaining the entire transmembrane and ligand-binding domains and so capable of producing the sFlt1 protein. *Flt1*$^{TK/TK}$ mice do not develop proteinuria or glomerular dysfunction out to 1.5 years of age, demonstrating that elimination of Flt1 signaling does not significantly alter podocyte function (Figures 2A and 2B; Table S1 available online). By contrast, 98% of mice lacking both full-length and soluble Flt1 proteins from podocytes (*Nphs1-Cre*$^{+}$*Flt1*$^{flox/flox}$) develop proteinuria and glomerular pathology by 6 weeks of age, as shown in Figures 1E and 2B and Table S1. To determine whether the selective presence of the kinase-deficient, truncated Flt1 in podocytes could rescue the phenotype, we generated mice carrying one TK allele, one floxed *Flt1* allele, and the *Nphs1*-Cre transgene (*Nphs1-Cre*$^{+}$*Flt1*$^{flox/TK}$). These mice can express full-length Flt1 as well as sFlt1 in all tissues except podocytes, in which the floxed allele is inactivated, leaving only *Flt1*^{TK}. Out of 33 animals that were examined, the majority (n = 25) do not develop proteinuria or other evidence of kidney pathology, indicating that a single *Flt1*^{TK} allele can rescue the kidney phenotype caused by deletion of *Flt1* from podocytes (Table S1). We isolated glomeruli from a group of *Nphs1-Cre*$^{+}$ *Flt1*$^{flox/TK}$ mice with (n = 3) or without (n = 12) abnormal proteinuria and measured *sFlt1* expression. Mice with proteinuria expressed lower levels of *sFlt1* (Figure 2C) compared with rescued *Cre*$^{+}$*Flt1*$^{flox/TK}$ mice, suggesting a threshold level of *sFlt1* is required to maintain normal podocyte morphology.

sFLT1 Promotes Cell Adhesion and Podocyte Cytoskeleton Reorganization

Our in vivo data suggest that elimination of sFlt1 in podocytes causes profound changes in structure and function, indicating a critical and unexpected function for sFlt1 in these cells. To explore the underlying mechanism, we assessed responses of human podocytes exposed to recombinant sFLT1. Podocytes adhere to native sFLT1 or sFLT1-Fc proteins with similar affinity as fibronectin, a strong stimulus of podocyte adhesion (Borza et al., 2008) (Figure 3A). Furthermore, there is a clear dose-dependence of the adhesive response to sFLT1 (Figure 3B). In contrast, podocytes do not attach to immunoglobulin G (IgG), sFLK1/KDR-Fc, or soluble platelet-derived growth factor receptor β-Fc (Figures 3A and 3B), confirming specificity of

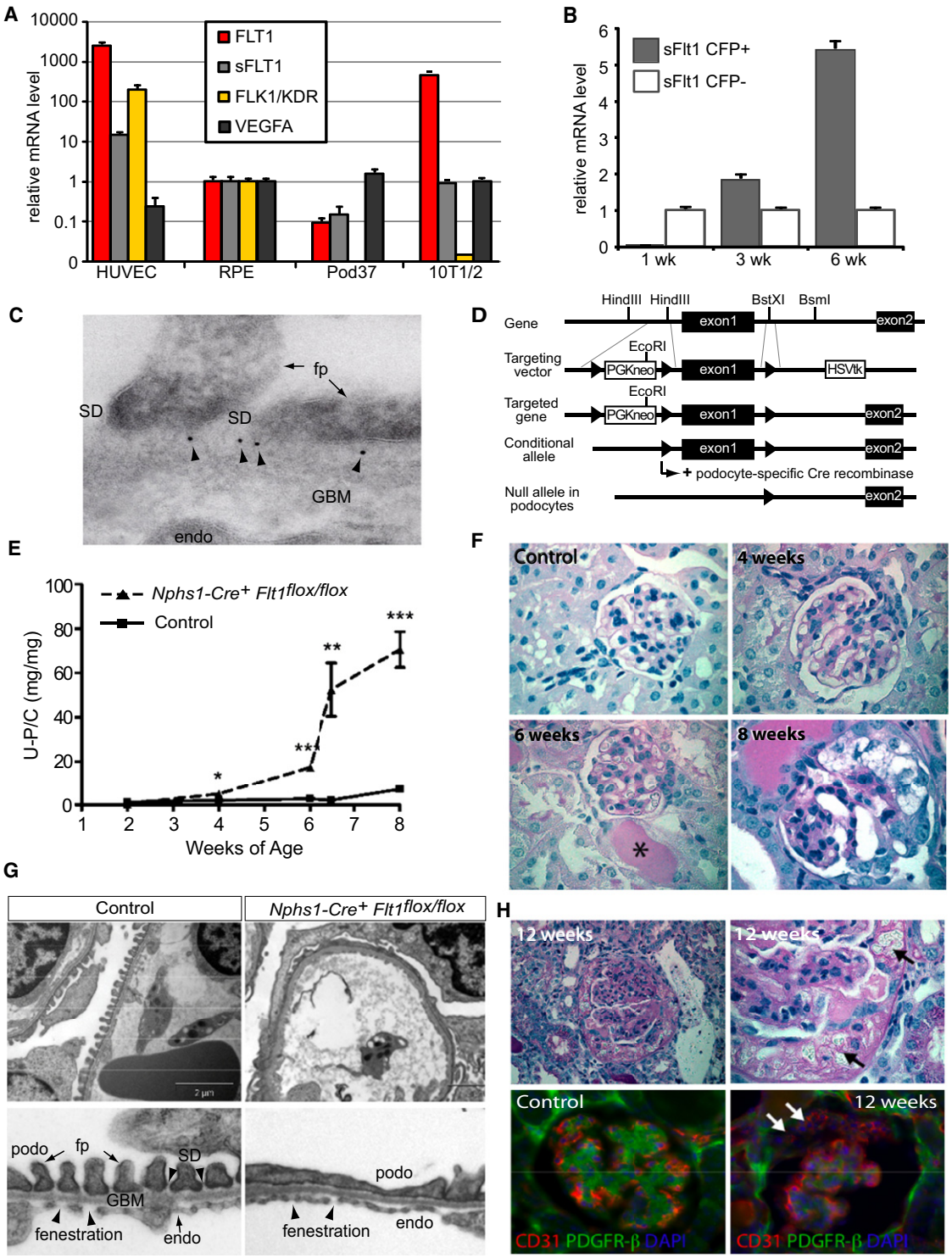

Figure 1. Deletion of *Flt1* from Podocytes Results in Foot Process Effacement and Proteinuria

(A) Similar to HUVECs, human perivascular cells and pericytes, including RPE cells, podocytes (Pod37) and 10T1/2 cells express full-length and soluble *FLT1* as determined by qPCR. mRNA levels were normalized to *HPRT*. Changes are shown as fold change compared to RPE expression (1) for each gene. Bars represent SEM.

(B) Mouse podocytes express *sFlt1* (measured by qPCR) beginning at 3 weeks of age and increasing until 6 weeks. Primary podocytes expressing a CFP+ transgene were isolated from mouse glomeruli. The CFP− fraction represents endothelial and mesangial cells isolated from the glomerulus. Expression levels are represented as normalized means and SEM.

reaction. We also monitored cell adhesion via real-time reading of electrical impedance (Yu et al., 2006). As expected, podocytes initiate attachment in response to sFLT1 more rapidly and with greater affinity than to sFLK1/KDR (Figure S1A). Adhesion of podocytes to fibronectin is cation dependent and mediated by αVβ3 integrins (Borza et al., 2008). While attachment of podocytes to sFLT1 is also inhibited by EDTA and EGTA, it is not affected by specific blocking antibodies to integrins (Figures S1B and S1C). Further, pretreatment with heparin has no effect on podocyte binding to fibronectin, but completely abolishes binding to sFLT1 in a dose-dependent manner (Figure 3C), suggesting a different mechanism of adhesion between the two substrates.

Finally, binding of podocytes to sFLT1 is accompanied by rapid and striking reorganization of the cytoskeleton with formation of filopodial or foot-process-like structures within minutes (Figure 3D).

sFLT1 Binds to the Cell Surface followed by Rapid Endocytosis

At 0°C, sFLT1 binds to the surface of podocytes in a fine punctate pattern (Figures 3E and S2A). Patching of sFLT1 on the cell surface is abolished by pretreatment of podocytes with heparin (Figure S2B). As before, there is no binding of sFLK1/KDR to podocytes (Figure S2A). Premixture with VEGF (biotinylated VEGF-165) does not affect sFLT1 binding to podocytes (Figure S2C). Also, in the absence of endogenous or exogenous VEGF, sFLT1 binding is not altered (data not shown), indicating this association is independent from the native ligand. Conversely, although there is no direct VEGF binding to the podocyte (data not shown), when VEGF is mixed with sFLT1 in the medium, we observed VEGF deposition on the cell surface at the sites of sFLT1 microdomains (Figure S2C) as well as VEGF endocytosis (data not shown), raising the possibility that sFLT1 might promote cellular uptake of VEGF.

Upon thermoshifting to 33°C, dynamic "pooling" or fusion of sFLT1 patches can be observed in real-time (Movie S1) followed by formation of distinct compact punctae (Figures 3E and S2A). The coalescence of punctae does not occur following treatment with dynasore, an inhibitor of dynamin (Figure S3A). At the plasma membrane, some of these punctae colocalize with flotillin and Rab5 (Figure S3B at 0°C), which are regulators of membrane dynamics and vesicle trafficking. Upon thermoshifting (Figure S3B at 33°C), the extent of colocalization is increased and most evident in endosomes. These sFLT1 punctae also colocalize with endocytic markers HRS1 and EEA1 (Figures S3A and S3C) and the endocytic/adaptor protein CIN85 (Figure S3D), consistent with rapid endocytosis of sFLT1 after binding. Immunogold staining demonstrates that, at 0°C, sFLT1 localizes to discrete patches on the surface of the podocyte, which expand at 33°C, suggesting coalescence of surface microdomains (Figure 3F). When cells are fixed 30 min after the addition of sFLT1, we find sFLT1 internalized in endocytic vesicles, and occasionally, immunogold-labeled sFLT1 is concentrated at the sites of cell-cell contact (Figure 3F).

Mass Spectrometry Analysis to Identify Binding Partners for sFLT1

Our data demonstrate specific interaction between the podocyte and sFLT1 at the cell surface, inducing adhesion and modification of the cytoskeleton. To identify sFLT1 binding partners on the podocyte cell surface, we utilized covalent crosslinking coupled with mass spectrometry. In a pilot study, we tested two crosslinkers, bissulfosuccinimidyl suberate (BS^3) and dimethyl adipimate (DMA). Only treatment with BS^3 produced sFLT1 bands at higher molecular weight (Figure S4A), and thus BS^3 was used for the large-scale mass spectrometry experiments.

sFLT1 and cross-linked proteins were immunoprecipitated from the lysate and digested with trypsin or chymotrypsin for mass spectrometry (Figure 4A). Coimmunoprecipitated proteins were identified and ranked according to mass spectrometry search scores (Mascot, Figure 4B). Three of the top hits, ANXA2, ROBO4, and SCARB1, were chosen for further study. ROBO4 partially colocalizes with sFLT1 in endocytic vesicles, whereas SCARB1 shows more extensive colocalization with sFLT1 on the surface of podocytes (Figure S3D). The cytoplasmic abundance of ANXA2 precludes membrane localization with any degree of certainty (data not shown). To determine if any of these proteins bind sFLT1, we performed coimmunoprecipitation studies but were unable to demonstrate direct interaction (data not shown), suggesting instead that they reside in a larger surface membrane complex with sFLT1.

sFLT1 Is Associated with the Lipid Raft

Although the initial goal of the screen was to identify a specific binding protein for sFLT1, we reasoned that proteins crosslinked due to their vicinity and abundance should provide useful

(C) Immunogold EM staining shows Flt1 (arrowheads) localizes to the base of the foot process (fp) and beneath the slit diaphragm (SD) of podocytes from rat kidneys. GBM, glomerular basement membrane.

(D) Targeting strategy for deletion of *Flt1* from podocytes. Triangles, loxP sites.

(E) Loss of *Flt1* from podocytes results in proteinuria determined by urine protein-creatine ratio (U-P/C) that starts at 4 weeks of age in *Nphs1-Cre+Flt1*$^{flox/flox}$ mice and increases rapidly with time. No proteinuria was observed in control mice. (*$p < 0.05$; **$p < 0.02$; ***$p < 0.01$). Bars represent SEM. See also Table S1.

(F) At 4 weeks of age, glomeruli from *Nphs1-Cre*$^{+}$*Flt1*$^{flox/flox}$ mice appear normal. At 6 weeks, protein is visible in the tubules (*), and by 8 weeks, glomerular structure is disrupted. A control glomerulus at 6 weeks is shown for comparison.

(G) At 6 weeks, podocytes from *Nphs1-Cre*$^{+}$*Flt1*$^{flox/flox}$ mutant mice show striking reorganization of cytoskeleton with foot process effacement. Compare to normal fp structure (left). Mutant animals exhibit flattening of podocyte foot processes, known as effacement. Endothelium is structurally intact, as evidenced by fenestrations (arrowheads).

(H) Abnormal blood vessel growth is observed in the urinary space of a minority of glomeruli (<5%) by 12 weeks of age. Red blood cells (black arrow) are visible in the ectopic vessels, which are lined by CD31+ endothelial cells (white arrows). PDGFRβ stains the mesangial cells. Compare to normal structure of control glomerulus in (F).

See also Table S1.

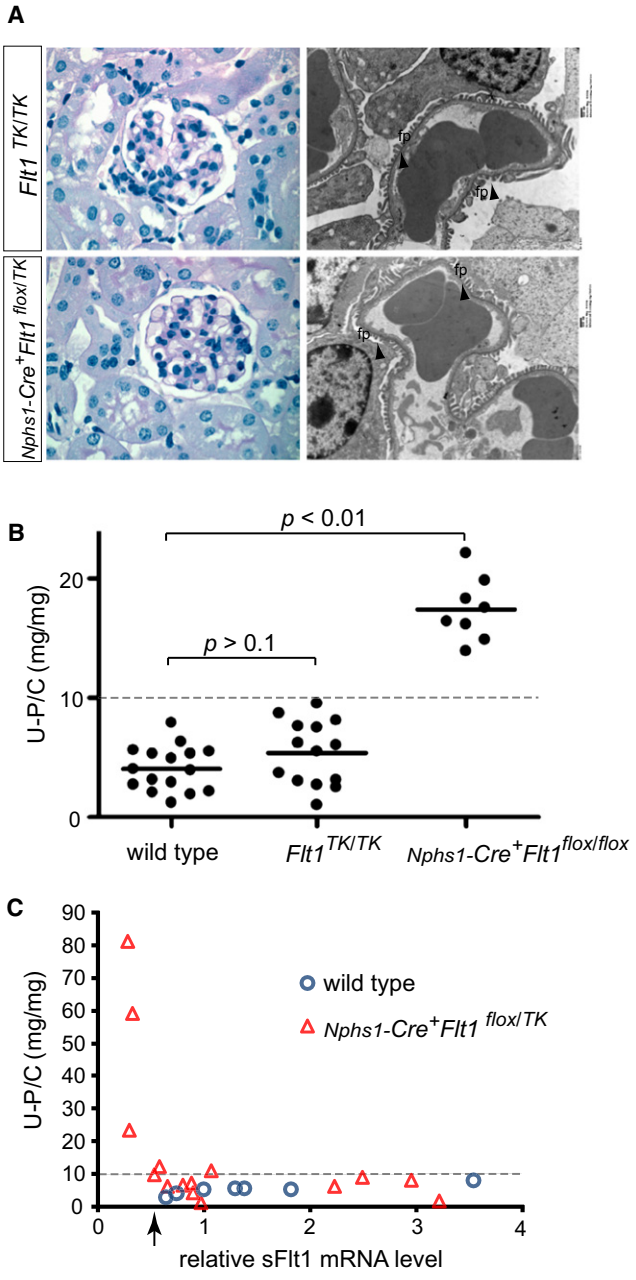

Figure 2. A Kinase-Deficient, Truncated *Flt1* Allele Rescues the Phenotype

(A) Glomeruli appear normal in *Flt1*$^{TK/TK}$ mutant mice up to 1.5 years of age (colored panels), and the ultrastructure of the glomerular barrier appears intact in transmission electron micrographs (black and white panels). A single TK allele rescues the podocyte defect in mice carrying one podocyte-specific null *Flt1* ^{flox} allele (*Cre*$^{+}$*Flt1*$^{flox/TK}$). Normal fps are indicated by arrowheads.

(B) U-P/C ratios are not different from wild-type in *Flt1*$^{TK/TK}$ mice, whereas *Nphs1-Cre*$^{+}$*Flt1*$^{flox/flox}$ littermates demonstrate elevated proteinuria at 6 weeks of age. Bars represent SEM.

(C) sFlt1 mRNA levels (determined by qPCR) are lower in the few *Nphs1-Cre*$^{+}$*Flt1*$^{flox/TK}$ mice that do not exhibit glomerular rescue (high U-P/C ratio), indicating a threshold level of sFlt1 is required for glomerular integrity. Measurements performed at 7 weeks of age.

See also Table S1.

clues about the molecular environment of sFLT1 at the cell surface. Of note, several of these proteins are known to localize to lipid raft microdomains. For example, Ca^{2+}-binding ANXA2 and its S100 subunit proteins have a structural role in the regulation of raft dynamics (Gerke et al., 2005) and SCARB1 is highly associated with raft microdomains, where it functions in the cholesterol uptake pathway (Rhainds et al., 2004). These proteomic findings are also consistent with the EM ultrastructural features of sFLT1-associated membrane patches, suggesting a raft-like dynamic (Figure 3F). Accordingly, we explored the association of sFLT1 with these proteins and the lipid raft itself. SCARB1 and sFLT1 are both isolated in the lipid raft fraction, defined by detergent resistance (Lingwood and Simons, 2010), the presence of caveolin-1, and absence of beta integrin (Figure 4C). Lipid rafts may also be identified by cholera-toxin B-subunit (CTxB) that binds to the raft ganglioside GM1. sFLT1 and CTxB demonstrate extensive colocalization on the plasma membrane of podocytes (Figure 4D).

Colocalization studies of sFLT1 with ANXA2 are not feasible, due to a lack of specific reagents. However, small interfering RNA (siRNA) knockdown of ANXA2 in podocytes (Figures S4C–S4E) alters the pattern and distribution of binding of CTxB and sFLT1 to the cell surface. At 0°C, CTxB and sFLT1 binding in the central region of the cells is completely absent (Figure 4E). Furthermore, ANXA2 knockdown causes major alterations in podocyte morphology, which is evident using phase contrast microscopy (Figures S4D and S4E). Together, these data suggest that ANXA2 serves as an integral component of the sFLT1-associated lipid raft surface complexes in podocytes.

sFLT1 Binds Directly to the Lipid Raft GM3 Ganglioside

GM3 is a second glycosphingolipid that is highly enriched in lipid raft domains, where it interacts with tyrosine kinase growth factor receptors, such as FLK1/KDR, and facilitates biologic responses in cells (Chung et al., 2009; Mukherjee et al., 2008). Given the high degree of sequence and structural conservation between FLT1 and FLK1/KDR, we reasoned that sFLT1 might also interact with GM3. Furthermore, the sialic acid moiety of GM3 exhibits a similar structure and negative charge as heparin, whereas sFLT1 is highly basic and carries a positive charge suggestive of electrostatic interactions between these molecules (Figure S5). In keeping with this possibility, heparin completely abolishes sFLT1 patching on the podocyte cell surface (Figure S2B). To determine whether GM3 interacts directly with sFLT1, we mixed purified GM3 with sFLT1-Fc or IgG affinity beads and determined the amount of GM3 bound to beads by mass spectrometry using multiple reaction monitoring (MRM). sFLT1 binds with 20-fold higher affinity to GM3 than IgG control (Figure 5A), confirming a direct interaction.

Having established the MRM protocol for GM3, which measures the ionization of the sialic acid group (Figure S6A), we extended the assay to monitor multiple ganglioside species simultaneously extracted from podocytes. Because gangliosides are characterized by the unique configuration of their sialated termini, allowing them to be systematically targeted by MRM, we programmed the mass spectrometer to detect 39 species of gangliosides. First, we demonstrated that it is possible to measure each of eight ganglioside types in a mixture of GM1,

GM3, and GD1a standards (Figure S6). We then conducted co-precipitation assays using sFLT1 and a crude extract of total gangliosides isolated from cultured podocytes; we used MRM to measure the binding of sFLT1 to each of the 39 individual ganglioside species (scheme in Figure 5B). This "lipidomic" approach identified GM3 as the predominant ganglioside species in podocytes, which binds with significantly higher affinity to sFLT1 than IgG controls. (Figures 5A and 5C; Table S2). Further, we tested whether enzymatic removal of sialic residues from gangliosides at the cell surface would affect cell binding to sFLT1. We treated cells with neuraminidase that cleaves sialic acid from the head group of the ganglioside and then performed cell adhesion assays. Neuraminidase treatment results in greater reduction of podocyte attachment to sFLT1 than to fibronectin (61% versus 26%, respectively) (Figure 5D). These results support a role for GM3 in mediating sFLT1 binding to the podocyte cell surface in the lipid rafts.

sFLT1 Binding Activates Intracellular Signaling Pathways

The observation that, at 0°C, sFLT1 binds to distinct membrane microdomains suggests the preexistence of these membrane entities independent of sFLT1 coalescence. However, the rapid and dramatic effect of sFLT1 binding on the podocyte cytoskeleton suggests activation of specific intracellular signaling pathways. Accordingly, we looked for transmembrane and intracellular molecules that might lead to signaling in response to sFLT1-induced raft dynamics.

The lipid raft-associated syndecan family of proteins is known to relay extracellular matrix (ECM) cues to intracellular signaling events that specifically regulate the actin cytoskeleton (Couchman, 2010; Morgan et al., 2007). Strikingly, syndecan 1 and 4 are localized to the exact membrane microdomains that bind sFLT1 (Figures 6A and S3D; data not shown), except at the cell-cell junctions that should be impermeable to exogenous sFLT1. Syndecans are major transmembrane heparin sulfate proteoglycans that play dual roles in ECM and cytoskeletal organization. Patching of sFLT1 induces rapid endocytosis of syndecan 1 (Figure S3D), reminiscent of endocytosis of ECM and $\alpha5\beta1$-integrin observed with syndecan 4 (Bass et al., 2011). In addition to the coreceptor functions of the ectodomains, syndecans signal through their short cytoplasmic tails, recruiting kinases and cytoskeletal regulatory proteins. Syndecans have a short C-terminal EFYA motif that binds the PDZ domains of cytoplasmic adaptor proteins (Figure 6B) and mediates a cooperative interaction with the tandem PDZ domains of syntenin. This interaction may couple syndecans to cytoskeletal targets and is blocked by tyrosine phosphorylation of the syndecan EFYA motif, thereby regulating actin dynamics (Grootjans et al., 1997; Sulka et al., 2009). To determine if sFLT1-mediated clustering of syndecans may be involved in regulating the cytoskeletal changes in podocytes following sFLT1 patching, we looked for tyrosine phosphorylation changes within the EFYA motifs of syndecan 1 and 4, using mass spectrometry. To overcome the limitations of mass-spectrometry analysis of tryptic fragments of phosphopeptides derived from the C-terminal end of proteins, we designed a Lys-N-digestion-based mass spectrometry protocol. This allowed us to directly identify syndecan EFYA phosphopeptides (Figures 6C, 6D, and S7). sFLT1 patching to the surface of podocytes caused increased phosphorylation of both syndecan 1 and 4 within their EFYA motifs, as judged by mass spectrometry (MS) (Figures 6D and S7B). As anticipated, phosphorylation of an EFYA-containing peptide from syndecan 1 blocks binding to the PDZ domains of syntenin (Figure 6E). Furthermore, knockdown of syndecan 1 and 4 from podocytes reduces adhesion of podocytes to sFLT1 (Figure 6G), but not to fibronectin. Together, these data suggest that syndecans may be among the transmembrane mediators of the actin dynamics induced by sFLT1 patching.

Nephrin (encoded by *NPHS1*) is a member of the immunoglobulin superfamily and constitutes a key component of a clinically relevant pathway controlling podocyte actin dynamics. Clustering of nephrin induces its tyrosine phosphorylation at three sites that bind the SH2/SH3 adaptor protein Nck, which in turn associates with actin regulators, such as N-Wasp (Blasutig et al., 2008; Jones et al., 2006). Nephrin tyrosine phosphorylation therefore leads to striking actin polymerization, important for the formation of podocyte foot processes and maintenance of the slit diaphragm. Moreover, nephrin is known to associate with caveolin-1-containing lipid rafts in podocytes. Thus, we sought to determine whether sFLT1 is involved in regulating phosphorylation of nephrin.

We find that sFLT1 colocalizes with nephrin in a podocyte cell line stably transfected with a plasmid expressing a MYC-tagged nephrin (Figure S3D). Exposure of podocytes to sFLT1 induces tyrosine phosphorylation of endogenous nephrin (Figure 6H), as nephrin phosphorylation is clearly seen following patching of sFLT1, while no phosphorylation is observed in an adjacent cell that has not incorporated sFLT1. Despite similar morphologic change, nephrin is not phosphorylated in podocytes following attachment to fibronectin (data not shown). To determine the physiological relevance of these findings to the in vivo setting, we examined expression of total and phosphorylated nephrin in *Nphs1-Cre*$^{+}$*Flt1*$^{flox/flox}$ mice. Nephrin tyrosine phosphorylation is lost at the onset of foot process effacement in *Nphs1-Cre*$^{+}$*Flt1*$^{flox/flox}$ mice, while total nephrin expression remains unchanged (Figure 6I). Western blot analysis demonstrates that dynamic sFLT1 binding to the cell surface correlates with a time-dependent phosphorylation of nephrin (Figure 6J). A model summarizing effects of sFLT1 patching on intracellular signaling events in the podocyte is shown in Figure 6K.

sFLT1 Promotes Rapid Adhesion of Pericytes and Perivascular Cells from Multiple Tissues

To investigate whether the functional properties of sFLT1 identified in podocytes are generalizable to pericytes from other tissues, we performed adhesion assays in a number of pericyte and perivascular cell lines, including placental pericytes, 10T1/2 embryonic fibroblasts/pericytes, retinal pigment epithelial (RPE) cells, and hepatic stellate cells (HSC). Similar to podocytes, we found that each of these cell lines adhere to sFLT in a heparin-dependent fashion (data not shown). Furthermore, there was patching of sFLT1 to the surface of pericytes, recapitulating the process we observed in podocytes (Figure 7A; data not shown). Patching was most striking in embryonic 10T1/2 pericytes, RPEs (Figure 7A), and HSCs (data not shown). RPEs

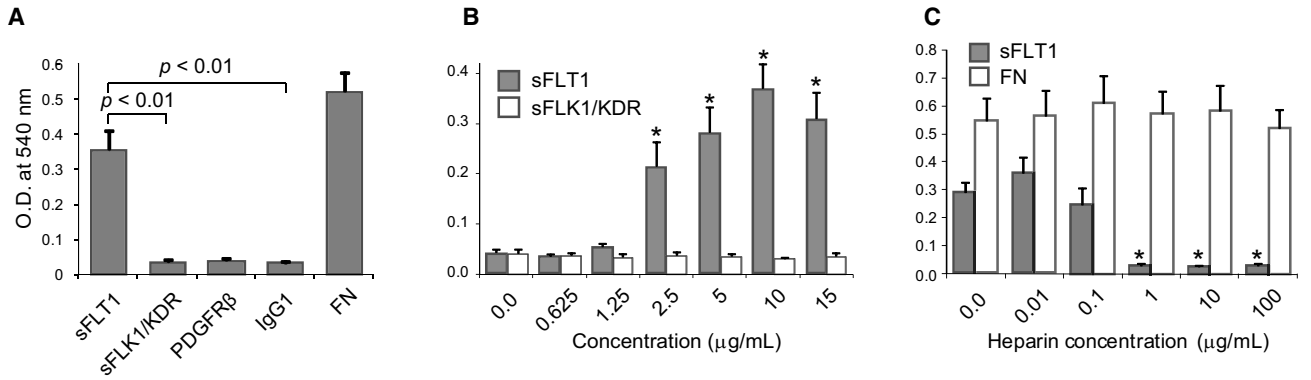
A
O.D. at 540 nm
p < 0.01
p < 0.01
sFLT1
sFLK1/KDR
PDGFRβ
IgG1
FN
B
sFLT1
sFLK1/KDR
Concentration (μg/mL)
C
sFLT1
FN
Heparin concentration (μg/mL)

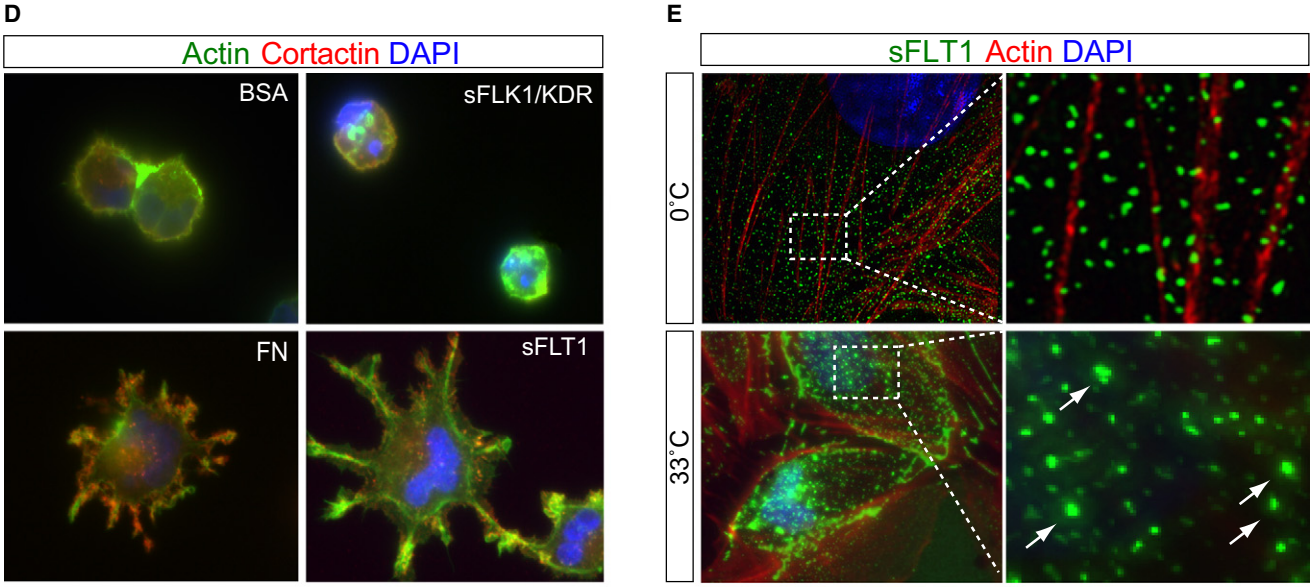
D
Actin Cortactin DAPI
BSA
sFLK1/KDR
FN
sFLT1
E
sFLT1 Actin DAPI
0°C
33°C

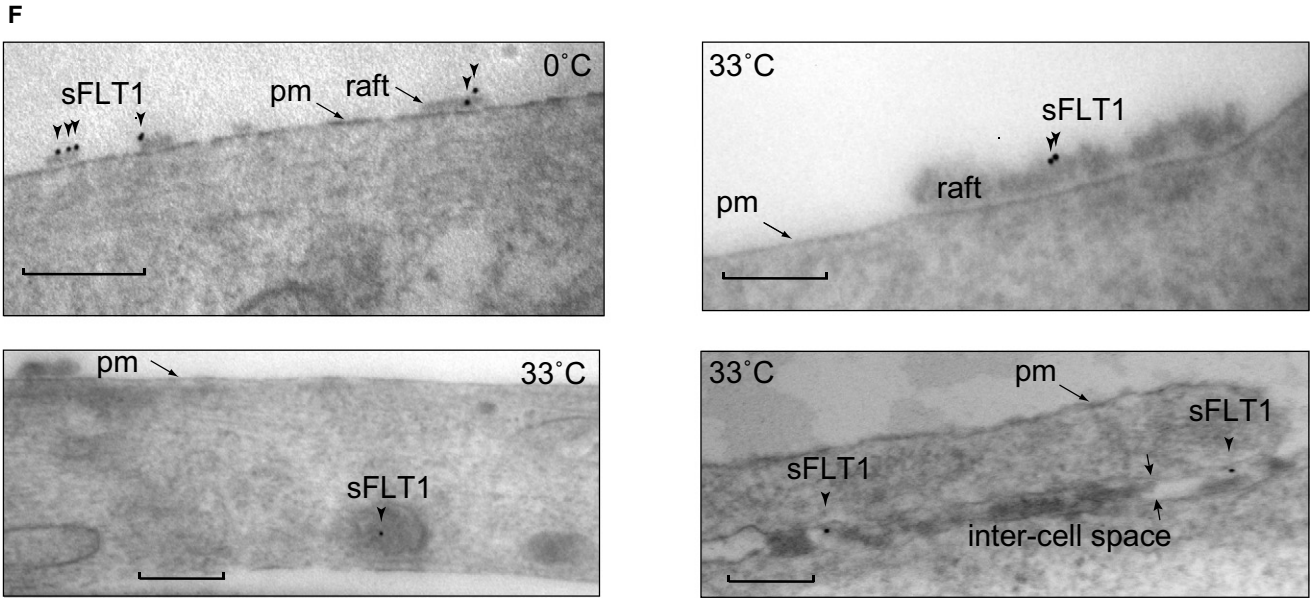
F
sFLT1
pm
raft
0°C
33°C
sFLT1
raft
pm
pm
33°C
sFLT1
33°C
pm
sFLT1
sFLT1
inter-cell space

are perivascular cells with many similarities to podocytes, including association with a fenestrated microvascular bed and constitutive expression of VEGF. By contrast, the pattern of patching was much weaker in primary glomerular endothelial cells (data not shown) and human umbilical vein endothelial cells (HUVECs) (Figure 7A) and dramatically different from podocytes, suggesting a different role for sFLT1 in endothelium. In RPEs, there was colocalization with syndecan 1 and 4 and internalization of this transmembrane protein upon sFLT1 binding similar to podocytes (data not shown), and neuraminidase treatment reduces attachment of RPEs to sFLT1 (data not shown). While our lipidomic analysis revealed some differences in surface gangliosides in RPEs compared to podocytes, GM3 is the predominant ganglioside type in both cells and binds to sFLT1 (data not shown).

FLT1 in Perivascular Cells Regulates Vascular Function in Multiple Tissues

To determine if Flt1 is also required in perivascular cells and pericytes outside the kidney to regulate vascular function, we crossed the *Flt1*$^{flox/flox}$ mice to the *Tcf21-Cre* mouse strain. Tcf21-Cre excises floxed alleles from embryonic mesenchymal cells that give rise to pericytes, perivascular cells, and interstitial cells in multiple tissues; these include podocytes, RPEs, HSCs, and pericytes of the trachea, retina, and lung (Maezawa et al., 2012). Importantly, this Cre-driver strain never excises from the endothelium. In addition to proteinuria and podocyte defects (data not shown), pericyte and vascular defects were also observed in extrarenal tissues, including the retina, trachea, lung, and liver. Mutant mice show increased vascularity and excessive vascular sprouts in retinas and tracheas at 4 weeks of age (Figures 7B and 7C). Excessive sprouting is associated with reduced pericyte coverage and presence of pericytes with abnormal morphology (Figure 7D).

DISCUSSION

Among the receptors for VEGF, the role of FLT1 is obscure. Its signaling function is dispensable in development and its soluble isoform, sFLT1, is best known as a decoy receptor that inhibits the proangiogenic effects of VEGF. For example, elevated circulating levels of sFLT1 are observed in patients with pre-eclampsia, resulting in endothelial dysfunction in multiple organs, including the glomerulus (Maynard et al., 2003). As many of the features of pre-eclampsia, such as proteinuria and hypertension, are recapitulated in patients who develop toxicity following treatment with anti-VEGF antibodies and in transgenic mouse models of VEGF knockdown, this decoy function of sFLT1 is well supported (Eremina et al., 2008). However, the role of sFLT1 in normal physiology is less clear. In healthy individuals, circulating levels of sFLT1 are low, but sFLT1 can be found localized to the extracellular matrix around healthy, fully differentiated blood vessels, suggesting that it may play a role in normal vascular biology (Sela et al., 2008).

Here we show that perivascular cells and pericytes that support endothelial cells in various tissues produce sFLT1. Deletion of *Flt1* from one population of specialized pericytes, the glomerular podocytes, in mice causes profound reorganization of the podocyte actin cytoskeleton and proteinuria, reflecting pericyte dysfunction. This proteinuria first manifests at 4 weeks of age and increases rapidly, coincident with the normal kinetics of *sFlt1* expression by podocytes. The soluble isoform of Flt1 seems to be critical for these actions, as mice carrying a kinase-deficient, truncated version of the *Flt1* allele (*Flt1*$^{TK/TK}$), which is unable to signal in a conventional manner, have normal kidneys and do not develop albuminuria. Furthermore, the *Flt1*^{TK} allele rescues the phenotype of *Flt1*-deficiency in podocytes, underscoring the importance of the sFlt1 and/or transmembrane portion of the molecule rather than Flt1 signaling in maintaining normal podocyte function.

Although the embryonic development of podocytes is unaffected in *Nphs1-Cre*$^{+}$*Flt1*$^{flox/flox}$ mice, their podocyte foot processes exhibit flattening by 5–6 weeks of age. Such dramatic reorganization of foot processes, known as effacement, is observed in primary and acquired proteinuric glomerular diseases. Similar to patients with nephrotic syndrome, loss of normal foot process structure in mice lacking Flt1 results in massive protein leakage into the urine due to disruption of the glomerular permeability barrier, resulting eventually in kidney failure.

How does loss of sFLT1 impact cytoskeletal regulatory pathways in pericytes? Given the profound defect in podocytes without apparent abnormalities in other glomerular cell types, we speculated that sFLT1 may function in an autocrine fashion to modulate pericyte function. In keeping with this model, we

Figure 3. sFLT1 Promotes Cell Adhesion and Podocyte Cytoskeleton Reorganization and Is Rapidly Endocytosed

(A) Podocytes adhere to sFLT1 with a similar affinity as to fibronectin (FN). Podocytes do not adhere to sFLK1/KDR, PDGFRβ, or IgG1 controls. O.D. represents optical density at 540 nm. Bars represent SEM.

(B) Adhesion to sFLT1 is dose dependent. Concentration of sFLT1 is shown on the x axis. *$p < 0.01$ from sFLT1 concentration at 0.0 μg/ml. Bars represent SEM.

(C) Heparin abolishes adhesion to sFLT1 in a dose-dependent manner, but not to fibronectin, suggesting a different mechanism of attachment. (*$p < 0.01$). Bars represent SEM.

(D) Upon attachment to sFLT1 at 33°C, human podocytes demonstrate dramatic morphologic change with extension of processes from the cell body, marked with cortactin (red), phalloidin (green), and DAPI (blue). No such change occurs when plated on sFLK1/KDR. Reorganization of the actin cytoskeleton of podocytes when bound to sFLT1 is similar but not identical to alteration on fibronectin.

(E) At 0°C, sFLT1 is bound in a specific pattern to small patches on the podocyte cell surface. Upon thermoshifting to 33°C (bottom), sFLT1 patches become compact and discrete (white arrows).

(F) Immunogold EM demonstrates that binding of sFLT1 starts at "fluffy" discrete patches on the podocyte cell surface (0°C, arrowheads show gold particles, upper-left). At 33°C, the sizes of labeled patches expand extensively, following the surface contour (upper-right). At this temperature, sFLT1 becomes visible inside cells within membrane-encapsulated structures suggestive of endosomes (lower-left). Immunogold-labeled sFLT1 also appears at sites of cell-cell contact between podocytes. sFLT1 can be observed filling the intercellular space (lower-right). pm, plasma membrane; raft, putative lipid raft.

See also Figures S1, S2, and S3 and Movie S1.

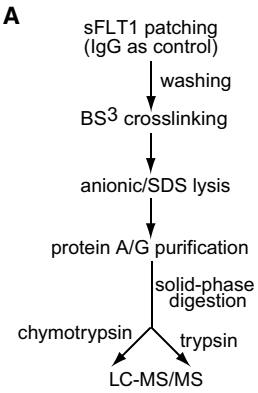

B

Rank	Protein name	Mascot score	Notes
1	FLT1	291	bait
2	ANXA2	152	associated with lipid rafts
3	S100-A9	74	in complex with ANXA2
4	Serpin B12	72	Serpin peptidase inhibitor
5	Robo4	57	transmembrane receptor
6	SCARB1	51	HDL receptor
7	TMCO4	49	membrane protein
8	TMC4	48	channel protein
9	p90 autoantigen	47	membrane protein
10	C20orf117	45	
11	C9orf5	45	membrane protein

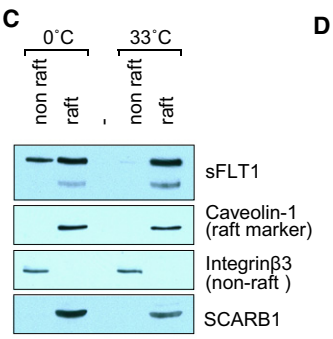

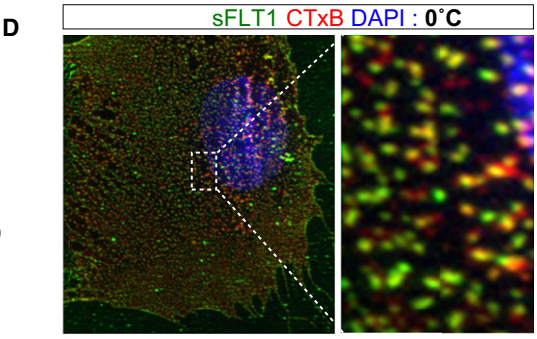

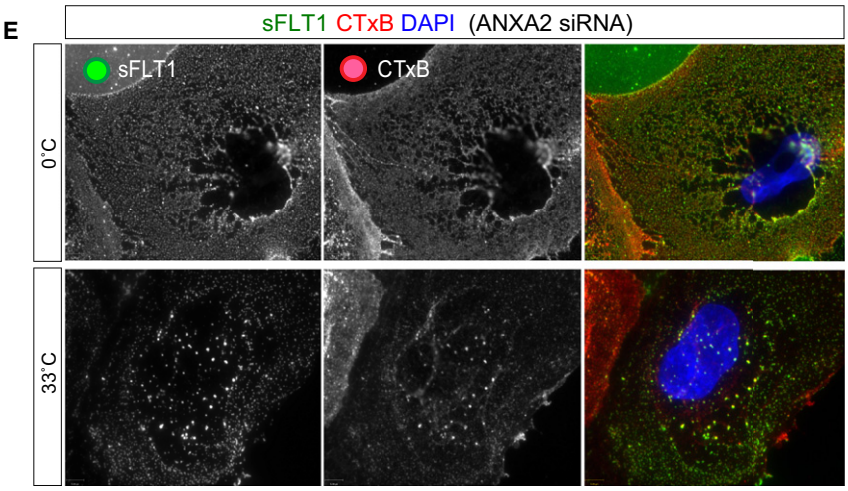

Figure 4. sFLT1 Associates with the Lipid Raft

(A) Cross-linking mass spectrometry protocol designed to identify proteins that bind to sFLT1 on the podocyte cell surface. Digestion with two enzymes was performed with chymotrypsin or trypsin.

(B) List of proteins for top peptide hits (defined by MASCOT score) identified in cross-linking mass spectrometry study. FLT1 had the highest score followed by a number of candidate membrane-associated proteins. See also Figure S3D.

(C) Isolation of detergent-resistant fraction from podocytes demonstrates that sFLT1 is localized to the lipid raft along with SCARB1 and caveolin-1. Integrinβ3 marks the nonraft component.

(D) sFLT1 extensively colocalizes with the CTxB that marks the lipid raft. Areas of sFLT1 (in green) and CTxB (in red) are indicated by varying shades of the yellow-orange composite color, which appear extensive (see close-up).

(E) Distribution and pattern of CTxB and sFLT1 binding is dramatically altered in ANXA2 knock-down podocytes, as CTxB rafts and sFLT1 are absent from the center area of cells (above the nucleus) as compared to controls (compare E to D). Top panels show sFLT1 patching at 0°C and bottom panels show patching at 33°C. See also Figure S4C and S4E.

See also Figures S3D and S4 and Movie S1.

observed dynamic patching and endocytosis of sFLT1 followed by rapid morphologic change of podocytes exposed to sFLT1, suggesting that sFLT1 binds to cell surface molecules. Utilizing a proteomics approach followed by colocalization studies, we identified a number of proteins that associate with sFLT1 at the cell surface. Intriguingly, two of the top hits, SCARB1 and ANXA2, are proteins known to associate with lipid rafts—subdomains involved in podocyte actin dynamics and in cytoskeletal reorganization in other pericyte populations (Simons et al., 2001; Sundberg et al., 2009). Along with their location in lipid rafts, these proteins were of interest for other reasons. First, SCARB1 is a scavenger receptor that binds molecules, such as apolipoproteins, facilitating their endocytosis. In addition, mutations in another member of the SCARB family, SCARB2, are associated with proteinuric glomerular disease and podocyte structural defects, although the mechanism(s) is not known (Balreira et al., 2008; Berkovic et al., 2008). ANXA2 controls actin cytoskeleton dynamics functioning as an actin-capping and actin monomer-binding protein in nonrenal cell types, including gut epithelium, where it regulates pedestal formation following insertion of the *E. coli* EPEC/Tir proteins; this process is highly analogous to nephrin-mediated foot process formation (Blasutig et al., 2008; Hayes et al., 2006; Zobiack et al., 2002). While we were unable to show direct interactions between sFLT1 and SCARB1 or ANXA2, we reasoned that their colocalization may reflect an association in the same molecular complex at the cell surface.

In support of this model, we showed that sFLT1 colocalizes with cholera toxin B and is present in the detergent-resistant membrane fraction together with SCARB1, arguing that sFLT1 binds to lipid rafts. We also showed that sFLT1 binds directly to the glycosphingolipid ganglioside GM3, a highly enriched component of lipid rafts that binds to a variety of growth factor

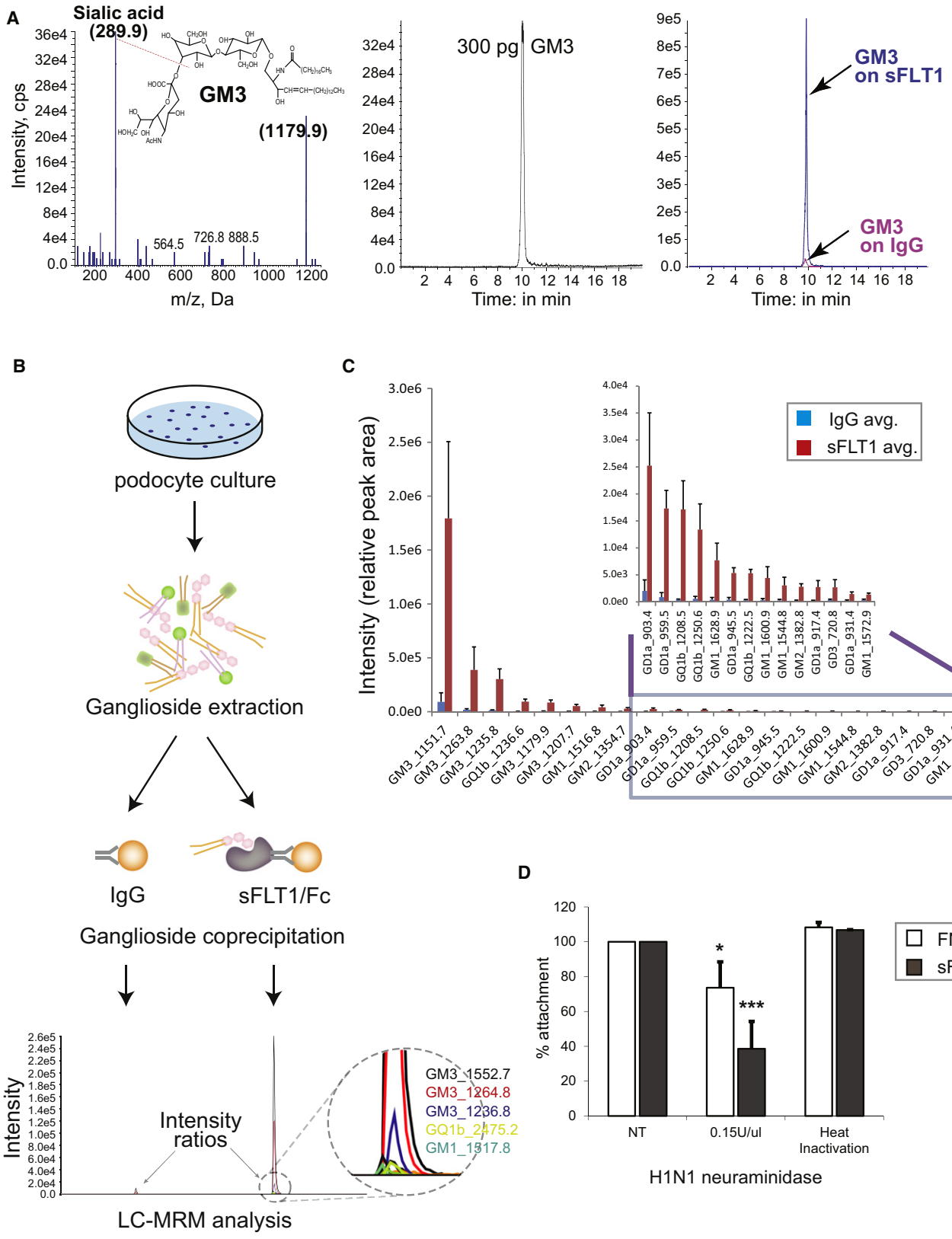
A
Sialic acid
(289.9)
GM3
(1179.9)
564.5
726.8 888.5
Intensity, cps
m/z, Da
300 pg GM3
Time: in min
GM3
on sFLT1
GM3
on IgG
Time: in min
B
podocyte culture
Ganglioside extraction
IgG
sFLT1/Fc
Ganglioside coprecipitation
Intensity
Intensity
ratios
GM3_1552.7
GM3_1264.8
GM3_1236.8
GQ1b_2475.2
GM1_1317.8
LC-MRM analysis
C
Intensity (relative peak area)
IgG avg.
sFLT1 avg.
GM3_1151.7
GM3_1263.8
GM3_1235.8
GQ1b_1236.6
GM3_1179.9
GM3_1207.7
GM1_1516.8
GM2_1354.7
GD1a_903.4
GD1a_959.5
GQ1b_1208.5
GQ1b_1250.6
GM1_1628.9
GD1a_945.5
GQ1b_1222.5
GM1_1600.9
GM1_1544.8
GM2_1382.8
GD1a_917.4
GD3_720.8
GD1a_931.4
GM1_1572.9
D
% attachment
FN
sFLT1
*
***
NT
0.15U/ul
Heat
Inactivation
H1N1 neuraminidase

receptors, facilitating signal transduction in other cells, such as T cells (Regina Todeschini and Hakomori, 2008).

Although it is not possible to genetically alter a single ganglioside in isolation, due to common steps in their synthesis, mutations in the major sialic acid biosynthesis enzyme *Gne*, which is required for proper GM3 synthesis, results in a profound glomerular defect and proteinuria in mice (Galeano et al., 2007), and reduced glomerular expression of the GM3 ganglioside has been linked to proteinuric kidney disease (Kwak et al., 2003). In this paper we demonstrate that GM3 is the most abundant ganglioside in podocytes and that removal of sialic acid residues with neuraminidase inhibits podocyte adhesion to sFLT1. These data support a functional role for GM3 in the filtration barrier and specifically in podocyte function.

There are several possible mechanisms governing the interactions between sFLT1 and GM3 in the lipid raft. The first is through direct carbohydrate-carbohydrate interactions, as has been reported for GM3 and EGFR (Yoon et al., 2006). In addition, we speculate that opposing electrostatic potentials between sFLT1 and GM3 may contribute to binding (Figures S5A and S5B). A sialic acid moiety constitutes the polar head of all gangliosides, including GM3, providing a negative charge (Figure S5B) and raising the possibility that sFLT1 may bind to other gangliosides present in the lipid raft. Similar to GM3, heparin also possesses a highly negative charge density (Figure S5C) and is known to bind to extracellular domains of VEGF receptors, including sFLT1 (Olsson et al., 2006; Park and Lee, 1999). It is plausible that heparin blocks sFLT1-mediated adhesion and raft clustering through charge interference with the sFLT1-GM3 interaction.

How might binding to the lipid raft result in changes in the actin cytoskeleton? Lipid rafts are highly dynamic domains within the cell membrane. Extracellular proteins that bind to these domains can promote coalescence or ''pooling'' of lipid-raft associated proteins into larger assemblies, allowing interactions to occur between signaling molecules that result in activation of specific intracellular signaling pathways (Figure 6K). Live imaging of podocytes showed rapid fusion of sFLT1 patches on the podocyte cell surface consistent with pooling of microdomains. Furthermore, binding of sFLT1 to the lipid raft causes striking morphologic changes and protrusion of foot process-like extensions from the podocyte cell body coincident with activation of intracellular signaling events that include nephrin phosphorylation.

In searching for candidate transmembrane proteins that might relay sFLT1-induced lipid raft dynamics to intracellular responses, we found members of the syndecan family of heparan sulfate proteoglycans, namely syndecan 1 and 4, are localized to the same membrane microdomains (Figures 6A and S3D; data not shown). Moreover, sFLT1 patching promotes coalescence and subsequent internalization of syndecan 1 and 4 (Figure S3D; data not shown) in a fashion similar to ECM-regulated cellular actions that occur through syndecan 4 (Bass et al., 2011), suggestive of a coclustering mechanism. The intracellular domain of syndecan is known to recruit signaling molecules, such as PKCα, and activate Src and focal adhesion kinase (FAK) tyrosine kinases upon ECM engagement (Couchman, 2010; Morgan et al., 2007). Thus, sFLT1 coalescence at the cell surface may cause the activation of Src and FAK pathways directly through syndecan, and this leads to the phosphorylation of nephrin in podocytes (Verma et al., 2006). Indeed, we show that phosphorylation of Tyr309 of syndecan 1 and Tyr197 of syndecan 4 are both increased upon sFLT1 patching (Figures 6D and S7). EFYA motifs of syndecans are known to recruit the PDZ domains of proteins that modulate intracellular signaling and cytoskeletal responses, and this binding is abrogated following syndecan phosphorylation (Sulka et al., 2009). We hypothesize that clustering of syndecans followed by phosphorylation of their EFYA motifs is a mechanism by which sFLT1 patching relays signals to induce cellular changes.

We find that sFLT1 is produced by other perivascular cell types, and attachment to sFLT1 is a general characteristic of pericytes from diverse lineages. Destabilization of pericyte-endothelial interactions, which is a prerequisite for sprouting angiogenesis, requires alteration of the cytoskeleton of perivascular cells and alterations in adhesion to underlying basement membrane. Our findings suggest that sFLT1 may be one pathway linking these two processes. In support of this model, deletion of FLT1 from extraglomerular pericytes and perivascular cells results in excessive sprouting angiogenesis in the retina and trachea and disrupted vasculature in multiple tissues.

In summary, our studies show that sFLT1 produced by pericytes has powerful autocrine functions to control cytoskeletal dynamics affecting their functions; elimination of FLT1 production by glomerular podocytes is sufficient to cause structural abnormalities, including effacement and loss of integrity of the glomerular barrier. We suggest that these functions are more broadly applicable to other specialized pericyte populations

Figure 5. Lipidomic Screen Using Mass Spectrometry Reveals sFLT1 Binding Predominately to GM3 Ganglioside

(A) (Left) MS/MS spectrum of a GM3 standard (extracted from brain)—the red dotted line to the structural formula indicates fragmentation for production of transition m/z 290.0 that, with the 1179.9 m/z parent ion, was used to build the MRM assay for quantitative mass spectrometry (middle). GM3 binds to sFLT1 with ~20-fold higher affinity than to IgG control as measured by MRM assay (right).

(B) Workflow for ganglioside extraction from cultured podocytes followed by measurement of affinities to sFLT1 by mass spectrometry. MRM was programmed to monitor 39 ganglioside species copurified with sFLT1 and IgG. Examples of obtained spectra are shown at the bottom. Lower affinity gangliosides are magnified (insert) to show levels.

(C) Twenty-two out of the 32 observed gangliosides from podocytes that showed enrichment and differential binding to sFLT1 are plotted (ranked by average intensity levels from four experimental repeats). The top three hits are all GM3 species, suggesting GM3 is the predominant ganglioside interacting with sFLT1. Bars represent SD.

(D) Treatment of podocytes with H1N1 neuraminidase reduces the level of cell attachment to sFLT1-coated surfaces. (*$p < 0.05$; ***$p < 0.01$, $n = 5$ independent experiments). Bars represent SEM.

See also Figures S5 and S6 and Table S2.

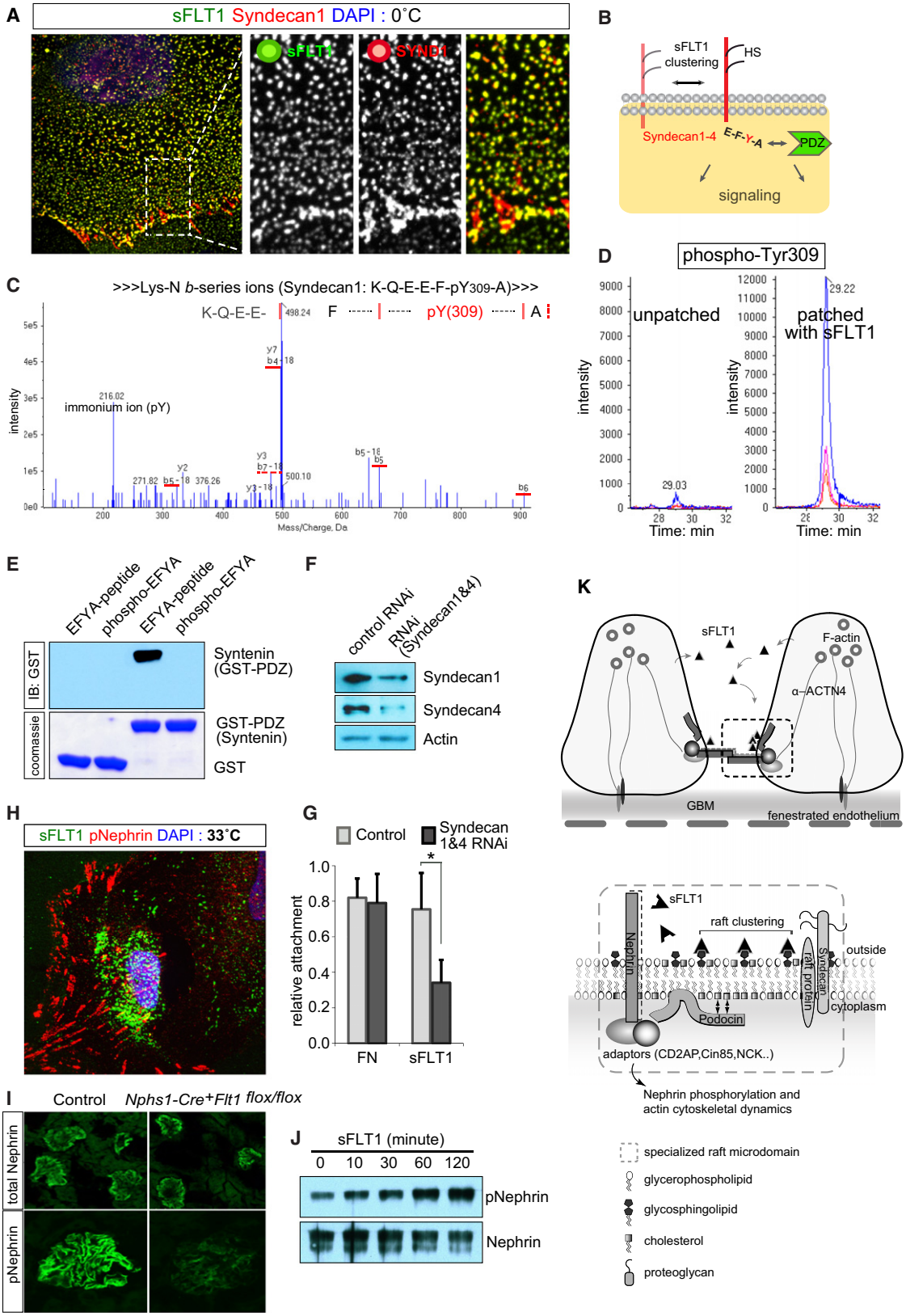
A
sFLT1 Syndecan1 DAPI : 0˚C
sFLT1
SYND1
B
sFLT1 clustering
HS
Syndecan1-4
E-F-Y-A
PDZ
signaling
C
>>>Lys-N b-series ions (Syndecan1: K-Q-E-E-F-pY309-A)>>>
K-Q-E-E-
498.24
F
pY(309)
A
intensity
immonium ion (pY)
216.02
Mass/Charge, Da
D
phospho-Tyr309
unpatched
patched with sFLT1
29.03
29.22
Time: min
E
EFYA-peptide
phospho-EFYA
IB: GST
coomassie
Syntenin (GST-PDZ)
GST-PDZ (Syntenin)
GST
F
control RNAi
RNAi (Syndecan1&4)
Syndecan1
Syndecan4
Actin
K
sFLT1
F-actin
α–ACTN4
GBM
fenestrated endothelium
H
sFLT1 pNephrin DAPI : 33˚C
G
Control
Syndecan 1&4 RNAi
relative attachment
FN
sFLT1
I
Control
Nphs1-Cre+Flt1 flox/flox
total Nephrin
pNephrin
J
sFLT1 (minute)
0 10 30 60 120
pNephrin
Nephrin
sFLT1
raft clustering
Nephrin
Podocin
adaptors (CD2AP,Cin85,NCK..)
Syndecan
raft protein
outside
cytoplasm
Nephrin phosphorylation and actin cytoskeletal dynamics
specialized raft microdomain
glycerophospholipid
glycosphingolipid
cholesterol
proteoglycan

and perivascular cells in mature vascular beds. Our findings suggest a paradigm for organization of the pericyte cytoskeleton that will be relevant to vascular biology and disease.

EXPERIMENTAL PROCEDURES

Transgenic Mice

Floxed Flt1 and Flt1 tyrosine kinase deficient (*Flt1*$^{TK/TK}$) mice have been described (Ambati et al., 2006; Hiratsuka et al., 1998). Cre driver strains used were: *Nphs1*-Cre (Eremina et al., 2002) and *Tcf21*- (Maezawa et al., 2012). See additional details in Extended Experimental Procedures.

Urine and Histologic Analysis

Details are provided in Extended Experimental Procedures.

Immunohistochemistry

Primary and secondary antibodies used on cells and tissue sections, together with detailed staining protocols, are provided in Extended Experimental Procedures.

FACS Sorting of Primary Podocytes

Glomeruli were isolated from 1-, 3-, and 6-week-old *Nphs1*–cyan fluorescent protein (CFP) transgenic mice by the sieving method (n = 3–5 mice in each age group). CFP-expressing podocytes were dissociated and separated by FACS analysis as previously described (Sison et al., 2010).

sFLT1 Patching Assay

Podocytes, RPEs, 10T1/2 cells, and HUVECs were grown on glass coverslips; binding of sFLT1 to the cell surface was allowed to proceed for 30 min at indicated temperature. Cells were fixed, permeabilized, blocked, and stained with indicated reagents following standard sample preparation protocol for immunofluorescence studies. VEGF, blocking studies, antibody details, and immunotransmission EM details are in Extended Experimental Procedures.

Crosslinking and Mass Spectrometry

Confluent podocytes grown in 500 cm^2 plates were incubated with either sFLT1-Fc recombinant protein or human IgG control antibody. After washing, BS^3 at 0.1 mM in phosphate buffer was added to the cells and the crosslinking reaction was allowed to proceed for 10 min. Total cell lysates were then collected and extracted with protein A- and protein G-sepharose beads to purify sFLT1-Fc together with crosslinked binding proteins. Details of sample preparation, mass spectrometry analysis, and scoring are provided in Extended Experimental Procedures.

Affinity between sFLT1 and GM3 Ganglioside Measured by Mass Spectrometry

GM1, GM3, and GD1a ganglioside standards were incubated for 1 hr with protein A/G-sepharose beads that had been preabsorbed with either sFLT1-Fc or control human IgG. After extensive washes, GM3 bound to the beads was extracted with methanol and the GM3 assay was run on an liquid chromatography-tandem mass spectrometry (LC-MS/MS) system (additional details in Extended Experimental Procedures).

LC-MRM Analysis of Gangliosides

The GM3 assay was developed and run on a nano LC-MS/MS system (details in Extended Experimental Procedures). Global ganglioside profiling was developed and run on a normal LC-MS/MS system, consisting of an Agilent 1100 cap LC system and a 4000 QTRAP mass spectrometer (AB SCIEX, Toronto, Canada). Samples were loaded and separated on a TSK-Gel Amide 80 column (4.6 mm ID × 25 cm, 3 μm, Tosoh Bioscience, Montgomeryville, PA). The multiple reaction monitoring (MRM) assay was programmed with 39 ganglioside precursor ions and the most abundant ion product of sialic acid − m/z 290.0 (sialic acid minus a water molecule), according to previous report (Ikeda and Taguchi, 2010). Additional details are in Extended Experimental Procedures.

Syndecan Phosphorylation Studies Using Mass Spectrometry

The method to identify and quantify syndecan phosphorylation were adapted from a previous study (Bisson et al., 2011). Additional details, such as sample preparation and a Lys-N-based mass spectrometry protocol to detect and quantify C-terminal phosphorylation of syndecan 1 and 4, are provided in Extended Experimental Procedures. The assay on recombinant syntenin PDZ domain binding to peptides derived from the C-terminal sequences of syndecan 1 and 4 is also described in Extended Experimental Procedures.

SUPPLEMENTAL INFORMATION

Supplemental Information includes Extended Experimental Procedures, seven figures, two tables, and one movie and can be found with this article online at http://dx.doi.org/10.1016/j.cell.2012.08.037.

ACKNOWLEDGMENTS

We thank Doug Holmyard and Ken Harpal for EM and histology; Sarang Kulkarni, Steffen Lawo, and Laurence Pelletier for microscopy and imaging; Gerry Gish for peptide synthesis and lipid assays; Rick Bagshaw for mass spec advice and providing Lys-N enzyme; Moin Saleem for human podocyte cells; Jim Dennis, Andras Kapus, Johan van der Vlag, Roy Zent, Jin Gyoon

Figure 6. sFLT1 Binding Activates Intracellular Signaling Pathways

(A) sFLT1 binding to microdomains on the surface of podocytes that are marked by syndecan 1.

(B) A working model to show sFLT1 patching induces phosphorylation of the conserved EFYA motif of syndecan. This C-terminal EFYA motif mediates signaling though recruitment of PDZ domain-containing proteins.

(C) Hemagglutinin (HA)-tagged syndecan 1 was purified from podocytes that were patched with sFLT1. The protein was digested by Lys-N and analyzed by mass spectrometry (also in D). The resolving MS-MS spectrum map of a phospho-KQEEFpYA peptide is shown. Evidence for Y309 phosphorylation is presented by *b*-series (highlighted in red) and *y*-series ions (not highlighted).

(D) MRM assay quantifies the levels of phospho-Tyr309 (compare peak intensity and area) before and after sFLT1 patching.

(E) Top panel: Synthetic syndecan 1 peptide containing the C-terminal EFYA motif binds recombinant GST-PDZ (of syntenin) protein. The phospho-EFYA peptide does not bind syntenin. The bottom panel shows the expression of the syntenin domain and control GST protein.

(F) Syndecan knockdown in podocytes reduces syndecan 1 and 4 expression in human podocytes, as shown by western blot.

(G) Syndecan knockdown reduces podocyte adhesion to sFLT1, but not to FN in attachment assays. Bars represent SEM.

(H) Phosphorylation of endogenous nephrin seen in a podocyte following patching of sFLT1 at 33°C (cell on the left), while it does not occur in an adjacent cell that has a lower level of sFLT1 incorporation (cell on the right).

(I) Nephrin phosphorylation is decreased in *Nphs1-Cre*$^{+}$*Flt1*$^{flox/flox}$ *mice* at the onset of foot process effacement, while staining for total nephrin is unchanged.

(J) Western blot analysis shows time-dependent increase in nephrin phosphorylation upon exposure of podocytes to sFLT1.

(K) Hypothetical model to illustrate autocrine function of sFLT1 to regulate podocyte cytoskeleton. sFLT1 binds to GM3 in lipid rafts on the cell surface that also contain nephrin, podocin, syndecan, and other raft proteins, such as SCARB1 and ANXA2. Upon binding, adaptor proteins that include CIN85 are recruited to the lipid raft, resulting in coalescence and phosphorylation of syndecans and nephrin, culminating in actin cytoskeletal changes.

See also Figure S7.

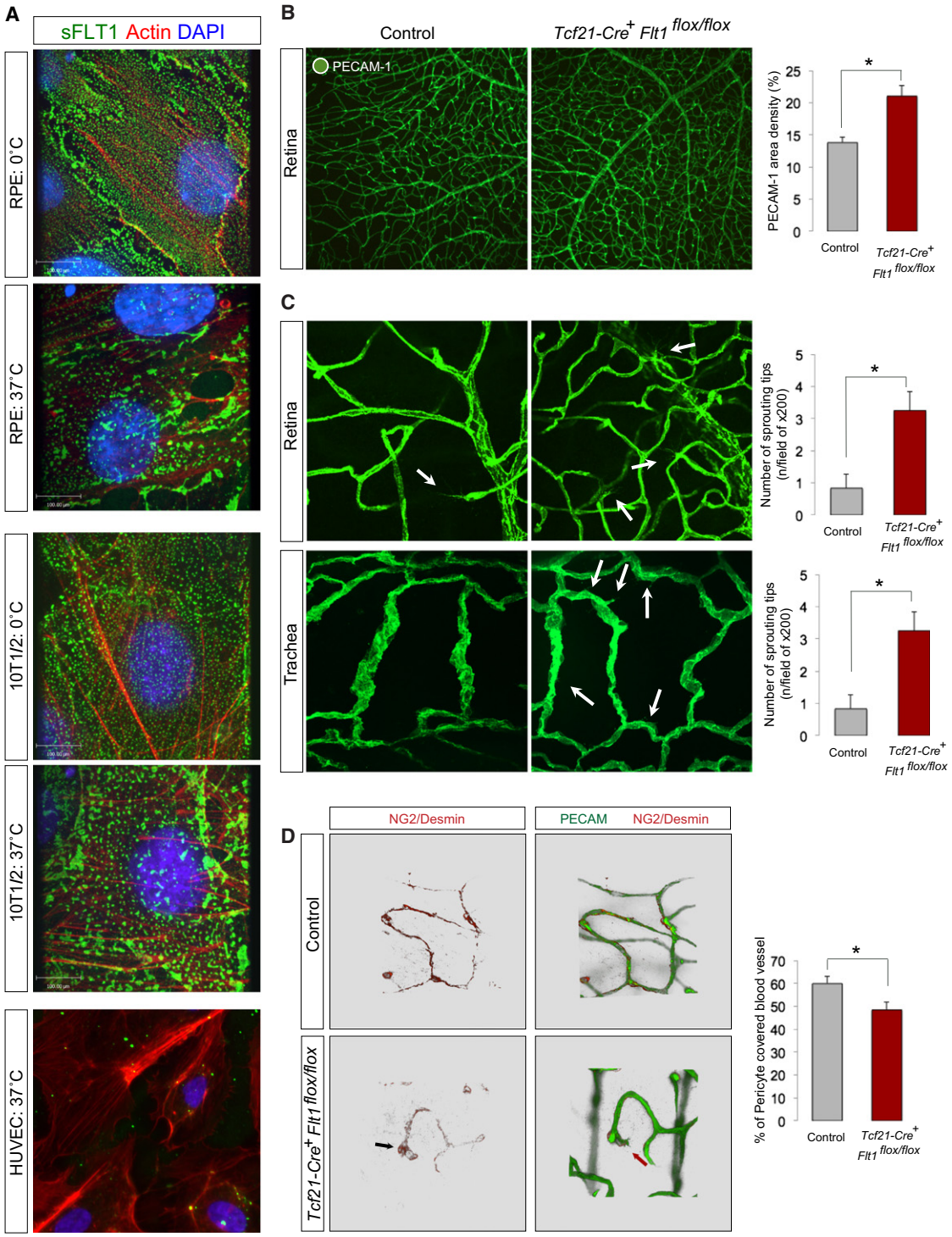

Figure 7. sFLT1 Regulates Function of Pericytes and Perivascular Cells from Nonrenal Vascular Beds

(A) RPEs and 10T1/2 pericytes show similar sFLT1 patching to podocytes. In contrast, HUVECs show no patching of sFLT1. The antibody detects the Fc tag on sFLT1-Fc protein.

(B) Vascular density is increased in tissues, including retina, in *Tcf21Cre*$^{+}$*Flt1*$^{flox/flox}$ mutants (quantified in bar graph with SEM).

(C) Deletion of Flt1 from pericytes of retina and trachea leads to increased vascular sprouting (white arrows; quantified in bar graph with SEM) at 4 weeks of age.

(D) A sprout is shown adjacent to a pericyte with abnormal morphology in retina from a *Tcf21Cre*$^{+}$*Flt1*$^{flox/flox}$ mutant mouse. Pericyte coverage is reduced in vessels from mutant mice (quantified in the bar graph with SEM).

Park, and Sergio Grinstein for helpful discussions; and Vivian Nguyen, Bret Larsen, and Lorne Taylor for technical assistance. This work was funded by CIHR grant MOP62931, TF grant 016002 to S.E.Q., who holds the Gabor-Zellerman Chair, CIHR-MOP57793 and HFSP-RGP0039/2009-C grants to T.P., CIHR- MOP-49409 to I.G.F., and TF grant 016002, CCRI grant 2010-700465 to A.N. J.J. received a CIHR Postdoctoral Fellowship, N.J. received a KRESCENT Award, and M.W. a Swiss NSF Postdoctoral Grant.

Received: April 7, 2012
Revised: August 2, 2012
Accepted: August 31, 2012
Published: October 11, 2012

REFERENCES

Ambati, B.K., Nozaki, M., Singh, N., Takeda, A., Jani, P.D., Suthar, T., Albuquerque, R.J., Richter, E., Sakurai, E., Newcomb, M.T., et al. (2006). Corneal avascularity is due to soluble VEGF receptor-1. Nature *443*, 993–997.

Balreira, A., Gaspar, P., Caiola, D., Chaves, J., Beirão, I., Lima, J.L., Azevedo, J.E., and Miranda, M.C. (2008). A nonsense mutation in the LIMP-2 gene associated with progressive myoclonic epilepsy and nephrotic syndrome. Hum. Mol. Genet. *17*, 2238–2243.

Bass, M.D., Williamson, R.C., Nunan, R.D., Humphries, J.D., Byron, A., Morgan, M.R., Martin, P., and Humphries, M.J. (2011). A syndecan-4 hair trigger initiates wound healing through caveolin- and RhoG-regulated integrin endocytosis. Dev. Cell *21*, 681–693.

Berkovic, S.F., Dibbens, L.M., Oshlack, A., Silver, J.D., Katerelos, M., Vears, D.F., Lüllmann-Rauch, R., Blanz, J., Zhang, K.W., Stankovich, J., et al. (2008). Array-based gene discovery with three unrelated subjects shows SCARB2/LIMP-2 deficiency causes myoclonus epilepsy and glomerulosclerosis. Am. J. Hum. Genet. *82*, 673–684.

Bisson, N., James, D.A., Ivosev, G., Tate, S.A., Bonner, R., Taylor, L., and Pawson, T. (2011). Selected reaction monitoring mass spectrometry reveals the dynamics of signaling through the GRB2 adaptor. Nat. Biotechnol. *29*, 653–658.

Blasutig, I.M., New, L.A., Thanabalasuriar, A., Dayarathna, T.K., Goudreault, M., Quaggin, S.E., Li, S.S., Gruenheid, S., Jones, N., and Pawson, T. (2008). Phosphorylated YDXV motifs and Nck SH2/SH3 adaptors act cooperatively to induce actin reorganization. Mol. Cell. Biol. *28*, 2035–2046.

Borza, C.M., Borza, D.B., Pedchenko, V., Saleem, M.A., Mathieson, P.W., Sado, Y., Hudson, H.M., Pozzi, A., Saus, J., Abrahamson, D.R., et al. (2008). Human podocytes adhere to the KRGDS motif of the alpha3alpha4alpha5 collagen IV network. J. Am. Soc. Nephrol. *19*, 677–684.

Chung, T.W., Kim, S.J., Choi, H.J., Kim, K.J., Kim, M.J., Kim, S.H., Lee, H.J., Ko, J.H., Lee, Y.C., Suzuki, A., and Kim, C.H. (2009). Ganglioside GM3 inhibits VEGF/VEGFR-2-mediated angiogenesis: direct interaction of GM3 with VEGFR-2. Glycobiology *19*, 229–239.

Couchman, J.R. (2010). Transmembrane signaling proteoglycans. Annu. Rev. Cell Dev. Biol. *26*, 89–114.

Eremina, V., Wong, M.A., Cui, S., Schwartz, L., and Quaggin, S.E. (2002). Glomerular-specific gene excision in vivo. J. Am. Soc. Nephrol. *13*, 788–793.

Eremina, V., Sood, M., Haigh, J., Nagy, A., Lajoie, G., Ferrara, N., Gerber, H.P., Kikkawa, Y., Miner, J.H., and Quaggin, S.E. (2003). Glomerular-specific alterations of VEGF-A expression lead to distinct congenital and acquired renal diseases. J. Clin. Invest. *111*, 707–716.

Eremina, V., Jefferson, J.A., Kowalewska, J., Hochster, H., Haas, M., Weisstuch, J., Richardson, C., Kopp, J.B., Kabir, M.G., Backx, P.H., et al. (2008). VEGF inhibition and renal thrombotic microangiopathy. N. Engl. J. Med. *358*, 1129–1136.

Fong, G.H., Rossant, J., Gertsenstein, M., and Breitman, M.L. (1995). Role of the Flt-1 receptor tyrosine kinase in regulating the assembly of vascular endothelium. Nature *376*, 66–70.

Galeano, B., Klootwijk, R., Manoli, I., Sun, M., Ciccone, C., Darvish, D., Starost, M.F., Zerfas, P.M., Hoffmann, V.J., Hoogstraten-Miller, S., et al. (2007). Mutation in the key enzyme of sialic acid biosynthesis causes severe glomerular proteinuria and is rescued by N-acetylmannosamine. J. Clin. Invest. *117*, 1585–1594.

Gerke, V., Creutz, C.E., and Moss, S.E. (2005). Annexins: linking Ca2+ signalling to membrane dynamics. Nat. Rev. Mol. Cell Biol. *6*, 449–461.

Grootjans, J.J., Zimmermann, P., Reekmans, G., Smets, A., Degeest, G., Dürr, J., and David, G. (1997). Syntenin, a PDZ protein that binds syndecan cytoplasmic domains. Proc. Natl. Acad. Sci. USA *94*, 13683–13688.

Hayes, M.J., Shao, D., Bailly, M., and Moss, S.E. (2006). Regulation of actin dynamics by annexin 2. EMBO J. *25*, 1816–1826.

Hiratsuka, S., Minowa, O., Kuno, J., Noda, T., and Shibuya, M. (1998). Flt-1 lacking the tyrosine kinase domain is sufficient for normal development and angiogenesis in mice. Proc. Natl. Acad. Sci. USA *95*, 9349–9354.

Ikeda, K., and Taguchi, R. (2010). Highly sensitive localization analysis of gangliosides and sulfatides including structural isomers in mouse cerebellum sections by combination of laser microdissection and hydrophilic interaction liquid chromatography/electrospray ionization mass spectrometry with theoretically expanded multiple reaction monitoring. Rapid Commun. Mass Spectrom. *24*, 2957–2965.

Jones, N., Blasutig, I.M., Eremina, V., Ruston, J.M., Bladt, F., Li, H., Huang, H., Larose, L., Li, S.S., Takano, T., et al. (2006). Nck adaptor proteins link nephrin to the actin cytoskeleton of kidney podocytes. Nature *440*, 818–823.

Kwak, D.H., Rho, Y.I., Kwon, O.D., Ahan, S.H., Song, J.H., Choo, Y.K., Kim, S.J., Choi, B.K., and Jung, K.Y. (2003). Decreases of ganglioside GM3 in streptozotocin-induced diabetic glomeruli of rats. Life Sci. *72*, 1997–2006.

Lingwood, D., and Simons, K. (2010). Lipid rafts as a membrane-organizing principle. Science *327*, 46–50.

Maezawa, Y., Binnie, M., Li, C., Thorner, P., Hui, C.C., Alman, B., Taketo, M.M., and Quaggin, S.E. (2012). A new cre driver mouse line, tcf21/pod1-cre, targets metanephric mesenchyme. PLoS ONE *7*, e40547.

Maynard, S.E., Min, J.Y., Merchan, J., Lim, K.H., Li, J., Mondal, S., Libermann, T.A., Morgan, J.P., Sellke, F.W., Stillman, I.E., et al. (2003). Excess placental soluble fms-like tyrosine kinase 1 (sFlt1) may contribute to endothelial dysfunction, hypertension, and proteinuria in preeclampsia. J. Clin. Invest. *111*, 649–658.

Morgan, M.R., Humphries, M.J., and Bass, M.D. (2007). Synergistic control of cell adhesion by integrins and syndecans. Nat. Rev. Mol. Cell Biol. *8*, 957–969.

Mukherjee, P., Faber, A.C., Shelton, L.M., Baek, R.C., Chiles, T.C., and Seyfried, T.N. (2008). Thematic review series: sphingolipids. Ganglioside GM3 suppresses the proangiogenic effects of vascular endothelial growth factor and ganglioside GD1a. J. Lipid Res. *49*, 929–938.

Niida, S., Kondo, T., Hiratsuka, S., Hayashi, S., Amizuka, N., Noda, T., Ikeda, K., and Shibuya, M. (2005). VEGF receptor 1 signaling is essential for osteoclast development and bone marrow formation in colony-stimulating factor 1-deficient mice. Proc. Natl. Acad. Sci. USA *102*, 14016–14021.

Olsson, A.K., Dimberg, A., Kreuger, J., and Claesson-Welsh, L. (2006). VEGF receptor signalling - in control of vascular function. Nat. Rev. Mol. Cell Biol. *7*, 359–371.

Park, M., and Lee, S.T. (1999). The fourth immunoglobulin-like loop in the extracellular domain of FLT-1, a VEGF receptor, includes a major heparin-binding site. Biochem. Biophys. Res. Commun. *264*, 730–734.

Regina Todeschini, A., and Hakomori, S.I. (2008). Functional role of glycosphingolipids and gangliosides in control of cell adhesion, motility, and growth, through glycosynaptic microdomains. Biochim. Biophys. Acta *1780*, 421–433.

Rhainds, D., Bourgeois, P., Bourret, G., Huard, K., Falstrault, L., and Brissette, L. (2004). Localization and regulation of SR-BI in membrane rafts of HepG2 cells. J. Cell Sci. *117*, 3095–3105.

Sawano, A., Iwai, S., Sakurai, Y., Ito, M., Shitara, K., Nakahata, T., and Shibuya, M. (2001). Flt-1, vascular endothelial growth factor receptor 1, is a novel cell surface marker for the lineage of monocyte-macrophages in humans. Blood *97*, 785–791.

Sela, S., Itin, A., Natanson-Yaron, S., Greenfield, C., Goldman-Wohl, D., Yagel, S., and Keshet, E. (2008). A novel human-specific soluble vascular endothelial

growth factor receptor 1: cell-type-specific splicing and implications to vascular endothelial growth factor homeostasis and preeclampsia. Circ. Res. *102*, 1566–1574.

Sela, S., Natanson-Yaron, S., Zcharia, E., Vlodavsky, I., Yagel, S., and Keshet, E. (2011). Local retention versus systemic release of soluble VEGF receptor-1 are mediated by heparin-binding and regulated by heparanase. Circ. Res. *108*, 1063–1070.

Shibuya, M. (2001). Structure and dual function of vascular endothelial growth factor receptor-1 (Flt-1). Int. J. Biochem. Cell Biol. *33*, 409–420.

Simons, M., Schwarz, K., Kriz, W., Miettinen, A., Reiser, J., Mundel, P., and Holthöfer, H. (2001). Involvement of lipid rafts in nephrin phosphorylation and organization of the glomerular slit diaphragm. Am. J. Pathol. *159*, 1069–1077.

Sison, K., Eremina, V., Baelde, H., Min, W., Hirashima, M., Fantus, I.G., and Quaggin, S.E. (2010). Glomerular structure and function require paracrine, not autocrine, VEGF-VEGFR-2 signaling. J. Am. Soc. Nephrol. *21*, 1691–1701.

Sulka, B., Lortat-Jacob, H., Terreux, R., Letourneur, F., and Rousselle, P. (2009). Tyrosine dephosphorylation of the syndecan-1 PDZ binding domain regulates syntenin-1 recruitment. J. Biol. Chem. *284*, 10659–10671.

Sundberg, C., Friman, T., Hecht, L.E., Kuhl, C., and Solomon, K.R. (2009). Two different PDGF beta-receptor cohorts in human pericytes mediate distinct biological endpoints. Am. J. Pathol. *175*, 171–189.

Verma, R., Kovari, I., Soofi, A., Nihalani, D., Patrie, K., and Holzman, L.B. (2006). Nephrin ectodomain engagement results in Src kinase activation, nephrin phosphorylation, Nck recruitment, and actin polymerization. J. Clin. Invest. *116*, 1346–1359.

Yoon, S.J., Nakayama, K., Hikita, T., Handa, K., and Hakomori, S.I. (2006). Epidermal growth factor receptor tyrosine kinase is modulated by GM3 interaction with N-linked GlcNAc termini of the receptor. Proc. Natl. Acad. Sci. USA *103*, 18987–18991.

Yu, N., Atienza, J.M., Bernard, J., Blanc, S., Zhu, J., Wang, X., Xu, X., and Abassi, Y.A. (2006). Real-time monitoring of morphological changes in living cells by electronic cell sensor arrays: an approach to study G protein-coupled receptors. Anal. Chem. *78*, 35–43.

Zobiack, N., Rescher, U., Laarmann, S., Michgehl, S., Schmidt, M.A., and Gerke, V. (2002). Cell-surface attachment of pedestal-forming enteropathogenic E. coli induces a clustering of raft components and a recruitment of annexin 2. J. Cell Sci. *115*, 91–98.